
Contextual Feedback Loops: Amplifying Deep Reasoning with Iterative Top-Down Feedback

Jacob Fein-Ashley¹ Rajgopal Kannan² Viktor Prasanna¹

Abstract

Conventional deep networks rely on one-way backpropagation that overlooks reconciling high-level predictions with lower-level representations. We propose *Contextual Feedback Loops* (CFLs), a lightweight mechanism that re-injects top-down context into earlier layers for iterative refinement. Concretely, CFLs map the network’s prediction to a compact *context vector*, which is fused back into each layer via gating adapters. Unrolled over multiple feedback steps, CFLs unify feed-forward and feedback-driven inference, letting top-level outputs continually refine lower-level features. Despite minimal overhead, CFLs yield consistent gains on tasks including CIFAR-10, ImageNet-1k, SpeechCommands, and GLUE SST-2. Moreover, by a Banach Fixed Point argument under mild Lipschitz conditions, these updates converge stably. Overall, CFLs show that even modest top-down feedback can substantially improve deep models, aligning with cognitive theories of iterative perception.

1 Introduction

Deep learning architectures (LeCun et al., 2015) have achieved remarkable success in computer vision, natural language processing, and other domains. Typically, these models follow a *feed-forward* design: signals flow bottom-up from input to output in a single pass. Despite their effectiveness, purely feed-forward approaches can struggle when inputs are ambiguous or when contextual cues could help refine intermediate features.

Human perception, on the other hand, relies on both bottom-up signals and top-down feedback (Rao & Ballard, 1999; Friston, 2010). When we see something ambiguous, we use high-level expectations (e.g., object-level understanding) to re-check and clarify lower-level features. For instance, when reading a partially obscured street sign, we might initially misread a letter but then realize from surrounding context (the style of the sign or the known set of possible words) that our first guess is unlikely. We then “go back” and

re-interpret the letters, resolving ambiguity via top-down cues.

Motivated by these insights from cognitive science and neuroscience, we propose a general-purpose, lightweight mechanism called *Contextual Feedback Loops* (CFLs). CFLs explicitly introduce a *feedback* channel from the high-level output (or near-final features) to earlier layers, enabling iterative refinement of the network’s internal states.

At a high level, CFLs:

- Compute an initial forward pass to get an output,
- Project that output (or a late-layer feature) into a compact *context vector*, and
- Re-inject this context into each lower layer through small *feedback adapters*, refining their hidden states and improving the output in subsequent passes.

Trained end-to-end via backpropagation through time (BPTT), the network learns to use its own high-level context to correct and refine early-stage representations. In Section 4, we present experiments on CIFAR-10, SpeechCommands, GLUE SST-2, and ImageNet-1k, showing consistent gains from even a single additional feedback iteration.

Contributions.

- We propose **Contextual Feedback Loops (CFLs)**: a straightforward, efficient method to incorporate top-down context into standard deep networks, bridging the gap between feed-forward and feedback-driven inference.
- We provide an **iterative refinement** algorithm that operates over multiple passes, yielding improved representations and outputs with modest overhead.
- Through **empirical evaluation** on multiple datasets, we demonstrate the effectiveness of CFLs in both convolutional and transformer-based architectures.
- We **analyze hidden state evolution** to show how intermediate representations converge under repeated feedback, clarifying the mechanism by which CFLs reduce ambiguity.

2 Related Work

Predictive Coding and Neurocognitive Insights. Classical theories of human perception highlight the role of top-down feedback (Grossberg, 2017). *Predictive coding* (Rao & Ballard, 1999; Friston, 2010) in particular emphasizes iterative interactions between high-level generative models and lower-level sensory signals. Empirical and computational evidence suggests these feedback loops help resolve ambiguities and sharpen representations over time, offering a rich inspiration for machine learning. **Further reviews** of predictive coding can be found in (Spratling, 2017) which surveys various algorithms and connects them to active inference principles.

Recurrent and Feedback Connections in Deep Models. Feedback and recurrence have been explored in various forms in deep learning:

- **Adaptive Resonance Theory (ART)** (Grossberg, 2017): Employs recurrent resonant loops for stable category learning.
- **Recurrent/Bidirectional Networks** (Spoerer et al., 2017; Wen et al., 2018; Elman, 1990): Incorporate backward connections to refine hidden states over time.
- **Predictive Coding Networks** (Lotter et al., 2016; Choksi et al., 2021): Unroll iterative error correction between top-down predictions and bottom-up inputs.
- **Capsule Networks** (Sabour et al., 2017): Dynamically refine part-whole relationships via routing-by-agreement.
- **Wake-Sleep Algorithm** (Hinton et al., 1995): Provides an early example of top-down generative feedback for unsupervised learning.

While related, these approaches often focus on reconstructive feedback or specialized routing mechanisms. By contrast, *Contextual Feedback Loops (CFLs)* directly use the model’s *current output* (e.g., logits or high-level features) as a global context signal to guide all layers in a lightweight fashion.

Iterative Inference and Refinement. Several works unroll multiple iterations of inference, either for deeper networks or improved accuracy:

- **Feedback Networks** (Zamir et al., 2017): Repeatedly pass top-layer features back to lower layers for object detection.
- **Deep Equilibrium Models** (Bai et al., 2019): Treat infinite-depth networks as a fixed-point iteration.
- **Iterative Refinement for Denoising/Segmentation** (Guo et al., 2017; Ronneberger et al., 2015): Show performance gains by repeatedly refining pixel-wise predictions.
- **Recurrent Image Generation** (Gregor et al., 2015):

Demonstrates that iterative feedback can build complex images step by step via an RNN-based model.

CFLs share the intuition that multiple passes can improve feature quality but focus specifically on a *compact* context vector derived from global outputs, enabling straightforward integration into existing architectures.

3 Method: Contextual Feedback Loops (CFL)

In this section, we introduce *Contextual Feedback Loops (CFLs)*, a lightweight but powerful mechanism to re-inject high-level signals into earlier layers of a deep network, thus enabling iterative refinement of intermediate representations. Figure 1 gives a high-level overview of the CFL framework. We then describe a step-by-step iterative procedure (illustrated in Figure 2) that uses this feedback mechanism to progressively refine hidden states. Finally, we provide a convergence argument for this iterative procedure under suitable contractive assumptions, invoking the Banach Fixed Point Theorem.

3.1 Base Network

Let us start with a base network comprising L layers that map an input $\mathbf{x} \in \mathbb{R}^{d_x}$ to an output $\mathbf{y} \in \mathbb{R}^{d_y}$. Concretely,

$$\begin{aligned} \mathbf{h}^{(1)} &= f^{(1)}(\mathbf{x}), \\ \mathbf{h}^{(2)} &= f^{(2)}(\mathbf{h}^{(1)}), \\ &\vdots \\ \mathbf{y} &= f^{(L+1)}(\mathbf{h}^{(L)}), \end{aligned} \quad (1)$$

where $\mathbf{h}^{(l)}$ denotes the hidden state at layer l . This base network can be *any* modern architecture, including a CNN, a Transformer-based model, an RNN variant, or even a generative model.

3.2 Feedback Pathway and Context Vector

To enable top-down refinement, we introduce a learnable *projector* $g(\cdot)$ that transforms the network’s output \mathbf{y} (or a late-layer feature) into a *context vector* $\mathbf{z} \in \mathbb{R}^{d_z}$:

$$\mathbf{z} = g(\mathbf{y}). \quad (2)$$

In practice, d_z can be significantly smaller than the dimension of the intermediate hidden states, resulting in minimal overhead. We then use *feedback adapters* $\{\psi^{(l)}\}$ at each layer to fuse \mathbf{z} back into the hidden state:

$$\tilde{\mathbf{h}}^{(l)} = \psi^{(l)}(\mathbf{h}^{(l)}, \mathbf{z}), \quad (3)$$

where $\tilde{\mathbf{h}}^{(l)}$ is the updated representation for layer l .

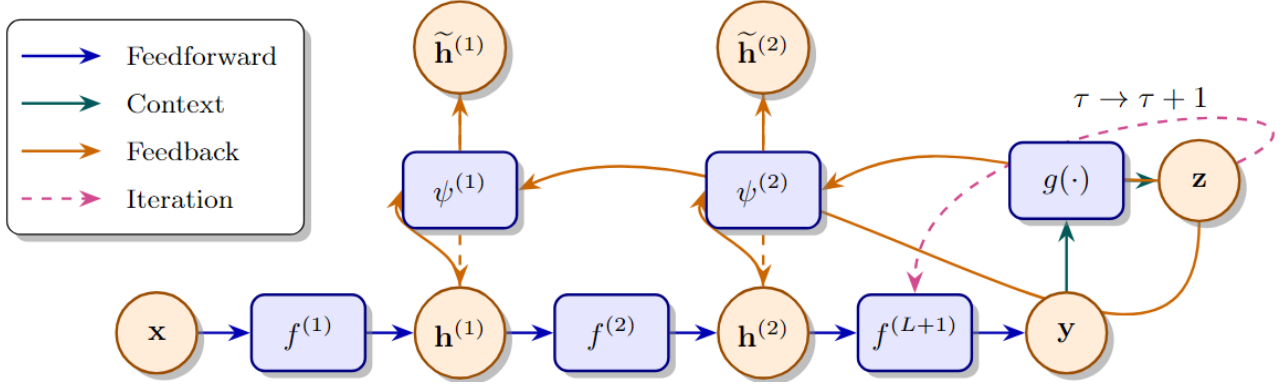


Figure 1. An overview of the Contextual Feedback Loops (CFL) framework. The top-level context vector is derived from the output and fed back to earlier layers, enabling iterative refinement.

3.3 Iterative Refinement

Figure 2 illustrates the unrolled *iterative* procedure. Rather than a single forward pass, CFLs allow repeated refinement steps:

1. **Initial forward pass:** Compute an initial output $\mathbf{y}^{(0)}$ and record the corresponding hidden states $\{\mathbf{h}_0^{(l)}\}$.
2. **Context computation:** Obtain a top-down context vector

$$\mathbf{z}^{(\tau)} = g(\mathbf{y}^{(\tau)}).$$

3. **Hidden state update:** For each layer $l \in \{1, \dots, L\}$,

$$\mathbf{h}_{\tau+1}^{(l)} = \psi^{(l)}(\mathbf{h}_{\tau}^{(l)}, \mathbf{z}^{(\tau)}).$$

4. **Output recomputation:** Pass the updated top layer state into the final function:

$$\mathbf{y}^{(\tau+1)} = f^{(L+1)}(\mathbf{h}_{\tau+1}^{(L)}).$$

5. **Repeat:** The process continues for $\tau = 0, 1, \dots, T - 1$, yielding progressively refined representations and outputs.

3.4 Gating Implementation

A practical way to implement $\psi^{(l)}$ is via a *gating mechanism*:

$$\gamma_{\tau}^{(l)} = \sigma(\mathbf{W}_g^{(l)}[\mathbf{h}_{\tau}^{(l)}; \mathbf{z}^{(\tau)}] + \mathbf{b}_g^{(l)}), \quad (4)$$

$$\tilde{\mathbf{h}}_{\tau}^{(l)} = \phi(\mathbf{W}_u^{(l)}[\mathbf{h}_{\tau}^{(l)}; \mathbf{z}^{(\tau)}] + \mathbf{b}_u^{(l)}), \quad (5)$$

$$\mathbf{h}_{\tau+1}^{(l)} = (1 - \gamma_{\tau}^{(l)}) \odot \mathbf{h}_{\tau}^{(l)} + \gamma_{\tau}^{(l)} \odot \tilde{\mathbf{h}}_{\tau}^{(l)}, \quad (6)$$

where $\sigma(\cdot)$ is a sigmoid function, $\phi(\cdot)$ is a suitable nonlinearity (e.g., ReLU or tanh), and \odot denotes elementwise multiplication. Intuitively, $\gamma_{\tau}^{(l)}$ decides how much to preserve from the old hidden state versus the new context-driven update.

3.5 Computational Complexity and Memory Overhead

Compared to a single-pass baseline network, CFL introduces two main sources of additional computational cost: **(i) Multiple refinement steps:** Performing T refinements effectively unrolls the network T times, but each unrolled step reuses the same weights. If a single forward pass of the base network requires $\mathcal{O}(C)$ compute (e.g., FLOPs), then naively, T refinements cost $\mathcal{O}(T \times C)$. However, in practice, some intermediate results (e.g., feature maps) can be cached, and partial recomputation can reduce overhead. **(ii) Feedback adapters and projector:** The additional parameters come from the gating/adapters $\psi^{(l)}$ and projector g . Since the context dimension d_z is typically much smaller than the hidden dimension, the parameter overhead is usually minimal (on the order of a few percent extra).

Overall, CFL trades off increased compute and memory for improved performance. In practice, we find that even small values of T (e.g., 2–3 refinements) often yield large gains, so the effective overhead remains manageable.

3.6 Training Objective

To train the network end-to-end with feedback, we apply backpropagation through time (BPTT) over the unrolled refinements. For a ground-truth label \mathbf{y}^* (in classification) or target output, we can define a multi-step loss:

$$\mathcal{L}(\theta) = \sum_{\tau=0}^T \lambda_{\tau} \ell(\mathbf{y}^{(\tau)}, \mathbf{y}^*), \quad (7)$$

where ℓ is typically cross-entropy, and λ_{τ} weights each iteration’s contribution. Setting λ_{τ} higher for later iterations encourages the final refinements to match ground truth more closely. All parameters of the base network, projector g , and adapters $\psi^{(l)}$ are learned jointly, enabling the model to discover how to *best* leverage top-down context to refine

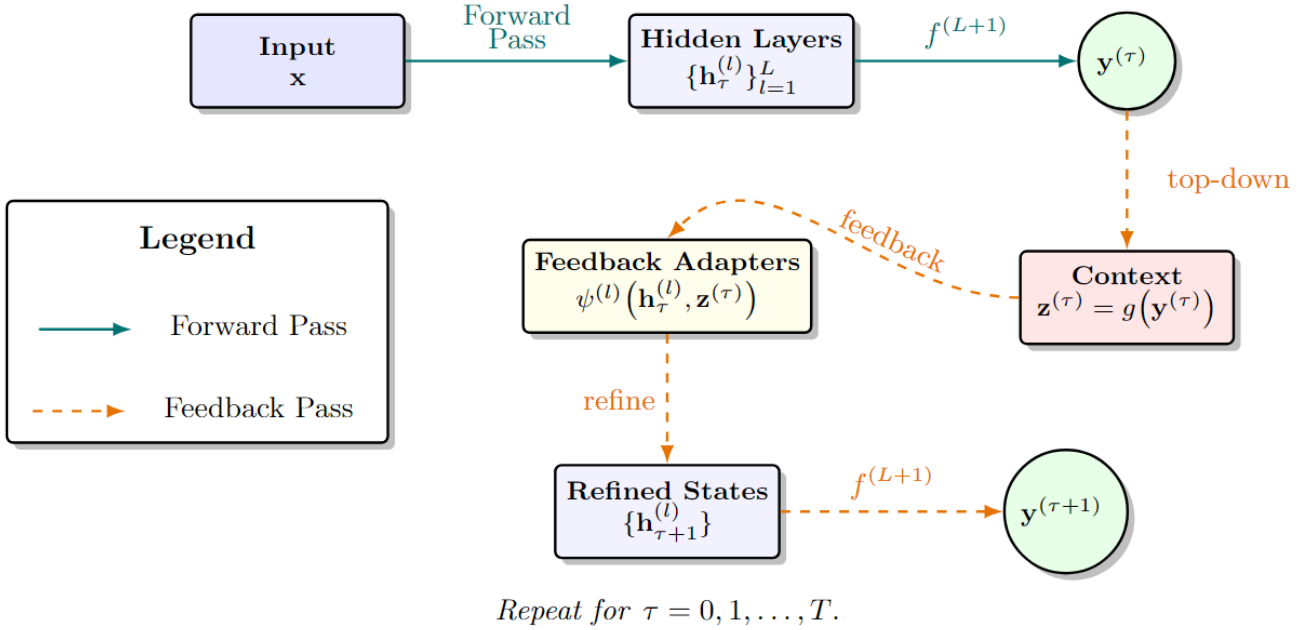


Figure 2. Schematic of the iterative refinement process for Contextual Feedback Loops (CFL). At each refinement step τ , the network produces an output $y^{(\tau)}$. A top-down context vector $z^{(\tau)}$ is computed and used by the feedback adapters to update hidden states, yielding refined representations $h_{\tau+1}^{(l)}$ and a new output $y^{(\tau+1)}$. This process repeats for T steps.

early-layer representations.

3.7 Architecture-Specific Integrations

CNNs. For convolutional architectures, each layer’s hidden state $h^{(l)}$ is typically a 3D tensor (height \times width \times channels). The feedback adapters can be small convolutions or fully connected layers (after a global pooling) that integrate the context vector z . This setup allows the model to fuse global feedback signals with local spatial features.

Transformers. In Transformers, the hidden states are sequences of token embeddings. The adapters $\psi^{(l)}$ can be integrated as an additional sub-layer (e.g., inserted after the multi-head attention or feed-forward layers). The context vector z can be broadcast across all tokens or appended as an extra token, enabling top-down refinement of attention mechanisms.

Recurrent Networks. For RNNs or LSTMs, CFL can be incorporated by augmenting each recurrent cell with an extra input z . The gating mechanism blends the RNN’s hidden state with feedback from the output. This effectively adds another recurrent connection from the output at time τ (or from a higher-level module) to the lower-layer states, enriching the temporal and hierarchical dynamics.

Generative Models. In VAEs, GANs, or autoregressive models, the “output” y could be the current generative distribution or the most recent sample. The context vector z derived from the output distribution can then refine earlier

latent features or generator layers. This iterative loop helps correct generation errors or align the model’s internal representation with the desired output distribution over multiple passes.

3.8 Implementation Details

Practically, one can implement CFL by:

- Adding a **projector** $g(\cdot)$ to produce z from the final output or an intermediate feature.
- Inserting **feedback adapters** $\psi^{(l)}$ at each layer, typically using a gating mechanism as shown in Section 3.4.
- Unrolling the network for T refinement steps, computing losses at each step (or only the final step, depending on the objective).
- Running BPTT through the unrolled graph to update both base and feedback parameters.

In our experiments, we often find $T = 2$ or 3 yields a good trade-off between performance and compute. Larger T can yield further improvements but may have diminishing returns (see Section 4.3 for a concrete example).

3.9 Fixed-Point Convergence via the Banach Theorem

Under suitable assumptions, the CFL iterative update can be viewed as a fixed-point iteration that converges to a unique

solution. Recall that by the Banach Fixed Point Theorem, an iterative sequence $\mathbf{S}_{\tau+1} = \Phi(\mathbf{S}_\tau)$ converges to a unique fixed point \mathbf{S}^* if there exists $c < 1$ such that

$$\|\Phi(\mathbf{S}) - \Phi(\mathbf{S}')\| \leq c \|\mathbf{S} - \mathbf{S}'\|, \quad (8)$$

for all \mathbf{S}, \mathbf{S}' in the underlying space. Convergence then follows from

$$\|\mathbf{S}_\tau - \mathbf{S}^*\| \leq c^\tau \|\mathbf{S}_0 - \mathbf{S}^*\|. \quad (9)$$

Setup. Define the state at iteration τ by

$$\mathbf{S}_\tau = (\mathbf{h}_\tau^{(1)}, \dots, \mathbf{h}_\tau^{(L)}, \mathbf{y}^{(\tau)}). \quad (10)$$

From Sections 3.2–3.3, each refinement induces a mapping Φ , given by:

$$\Phi(\mathbf{S}_\tau) = \left(\psi^{(1)}(\mathbf{h}_\tau^{(1)}, \mathbf{z}^{(\tau)}), \dots, \psi^{(L)}(\mathbf{h}_\tau^{(L)}, \mathbf{z}^{(\tau)}), \right. \\ \left. f^{(L+1)}(\mathbf{h}_{\tau+1}^{(L)}) \right), \quad (11)$$

where $\mathbf{z}^{(\tau)} = g(\mathbf{y}^{(\tau)})$.

Theorem 3.1 (Contractive Convergence of CFL). *Suppose each component function in Φ (i.e., each $\psi^{(l)}$, g , and $f^{(L+1)}$) is Lipschitz continuous and that their combined Lipschitz constants (when composed) can be made strictly less than 1. Formally, assume there exists a norm $\|\cdot\|$ and a constant $L < 1$ such that*

$$\|\Phi(\mathbf{S}) - \Phi(\mathbf{S}')\| \leq L \|\mathbf{S} - \mathbf{S}'\| \text{ for all } \mathbf{S}, \mathbf{S}'.$$

Then the sequence $\mathbf{S}_{\tau+1} = \Phi(\mathbf{S}_\tau)$ converges to a unique fixed point \mathbf{S}^* satisfying $\mathbf{S}^* = \Phi(\mathbf{S}^*)$.

Proof. We demonstrate that Φ is a contraction under mild network constraints.

Notation. Let

$$\mathbf{S}_\tau = (\mathbf{h}_\tau^{(1)}, \dots, \mathbf{h}_\tau^{(L)}, \mathbf{y}^{(\tau)}), \quad \mathbf{S}'_\tau = (\mathbf{h}'_\tau^{(1)}, \dots, \mathbf{h}'_\tau^{(L)}, \mathbf{y}'^{(\tau)})$$

We write $\mathbf{S}_{\tau+1} = \Phi(\mathbf{S}_\tau)$ and $\mathbf{S}'_{\tau+1} = \Phi(\mathbf{S}'_\tau)$.

Step 1: Relate changes in \mathbf{z} to changes in \mathbf{y} . Since $\mathbf{z}^{(\tau)} = g(\mathbf{y}^{(\tau)})$, and g is L_g -Lipschitz,

$$\|\mathbf{z}^{(\tau)} - \mathbf{z}'^{(\tau)}\| \leq L_g \|\mathbf{y}^{(\tau)} - \mathbf{y}'^{(\tau)}\|.$$

Step 2: Relate changes in hidden states to changes in \mathbf{z} .

At layer l , the updated state is

$$\mathbf{h}_{\tau+1}^{(l)} = \psi^{(l)}(\mathbf{h}_\tau^{(l)}, \mathbf{z}^{(\tau)}).$$

If $\psi^{(l)}$ is L_ψ -Lipschitz in both its arguments (with potentially separate constants for each argument that we combine into one for simplicity), then

$$\|\mathbf{h}_{\tau+1}^{(l)} - \mathbf{h}'_{\tau+1}^{(l)}\| \leq L_\psi \|\mathbf{h}_\tau^{(l)} - \mathbf{h}'_\tau^{(l)}\| + L_\psi \|\mathbf{z}^{(\tau)} - \mathbf{z}'^{(\tau)}\|.$$

Step 3: Relate changes in \mathbf{y} to changes in the top-layer state. Finally,

$$\mathbf{y}^{(\tau+1)} = f^{(L+1)}(\mathbf{h}_{\tau+1}^{(L)}),$$

and if $f^{(L+1)}$ is L_f -Lipschitz,

$$\|\mathbf{y}^{(\tau+1)} - \mathbf{y}'^{(\tau+1)}\| \leq L_f \|\mathbf{h}_{\tau+1}^{(L)} - \mathbf{h}'_{\tau+1}^{(L)}\|.$$

Combined contraction. By recursively applying these Lipschitz bounds from layer 1 up to L , we see that each step’s change is bounded by a factor $\underbrace{L_\psi \cdot L_\psi \cdot \dots \cdot L_f \cdot \dots}_{=: L_{\text{total}}}$

times the previous step’s change in \mathbf{S} . If we ensure (via weight initialization, normalization, or other spectral regularizations) that $L_{\text{total}} < 1$, then:

$$\|\mathbf{S}_{\tau+1} - \mathbf{S}'_{\tau+1}\| \leq L_{\text{total}} \|\mathbf{S}_\tau - \mathbf{S}'_\tau\|,$$

showing Φ is a contraction.

Banach Fixed Point Theorem. Once Φ is established as a contraction, the Banach Fixed Point Theorem guarantees a unique fixed point \mathbf{S}^* with $\mathbf{S}^* = \Phi(\mathbf{S}^*)$. Moreover, starting from any initial state \mathbf{S}_0 , the iterates satisfy

$$\|\mathbf{S}_\tau - \mathbf{S}^*\| \leq L_{\text{total}}^\tau \|\mathbf{S}_0 - \mathbf{S}^*\|,$$

implying geometric convergence to \mathbf{S}^* . \square

Discussion. In practice, strictly enforcing $L_{\text{total}} < 1$ (i.e., a contractive mapping) may require careful choices of weight initialization, normalization, and bounded activation functions. Even if Φ is not strictly contractive in theory, moderate regularization or small refinements ($T = 2, 3$) often suffice for stable behavior. This gives a theoretical underpinning for why a few feedback iterations can improve performance with minimal overhead.

4 Experiments

Our experiments aim to *isolate* the effect of top-down feedback for various backbone architectures (CNNs, Transformers, etc.). Rather than comparing a feedback-enabled CNN or ViT to an entirely different family of models, we compare each baseline *only* to the *same* architecture augmented with CFL. This approach ensures that any performance gains we observe are directly attributable to the top-down feedback mechanism itself, rather than confounding factors such as different network depths, specialized pretraining, or hyperparameter tweaks. By keeping the backbone fixed and only adding the feedback adapters, we obtain a clean, apples-to-apples comparison that highlights the contribution of feedback in each setting.

We also do not compare our approach directly to *predictive coding* or other biologically inspired feedback-based methods. While these methods share the broader notion of feedback, they typically involve specialized architectures or constraints that diverge significantly from common CNN/Transformer pipelines (e.g., different objective functions, inference loops, or biologically motivated design constraints). Such differences complicate direct comparisons. By focusing on a straightforward modification to standard deep networks, we aim to show that top-down feedback can be integrated simply and effectively into conventional architectures without additional specialized machinery.

We evaluate CFLs across four main benchmarks: CIFAR-10, SpeechCommands, ImageNet-1K, and GLUE (SST-2) (Wang et al., 2019).

4.1 Refinement Dynamics on CIFAR-10

We first demonstrate how top-down feedback progressively *stabilizes* hidden representations. Using a 3-layer CNN backbone on CIFAR-10:

1. We do an initial forward pass, recording each layer’s hidden states $\mathbf{h}_0^{(1)}, \mathbf{h}_0^{(2)}, \mathbf{h}_0^{(3)}$.
2. We compute $\mathbf{z}^{(0)} = g(\mathbf{y}^{(0)})$ and update all hidden states to $\mathbf{h}_1^{(l)}$.
3. We measure how much each hidden state changes across iterations via KL divergence and MSE.

Figure 4 shows that each layer’s representation changes most significantly in the early iterations, then gradually converges. By iteration 5, each layer has largely stabilized. This supports the hypothesis that *top-down signals mitigate ambiguity in the lower layers*, gradually aligning them with context gleaned from higher-level features.

4.2 Performance Comparison with a Standard CNN on CIFAR-10

We next compare a **FeedbackCNN** (CNN + CFL) against a standard CNN on CIFAR-10. Both models use the same backbone structure except for the feedback adapters. Figure 5 plots validation loss and accuracy over training epochs.

Results. The FeedbackCNN outperforms the regular CNN by about 3% in final test accuracy, and its validation loss remains consistently lower throughout training. Table 1 reports multiple-run accuracy for both models; the difference is statistically significant ($p < 0.01$).

4.3 Effect of Refinement Iterations on CIFAR-10

A key hyperparameter in CFL is the number of *refinement steps* T . Table 2 shows how final test accuracy on CIFAR-10 improves as we increase T from 1 to 5 in the FeedbackCNN model. Each refinement iteration updates the hidden states

Model	Run 1	Run 2	Run 3	Run 4	Run 5
CNN	75.1	75.4	74.8	76.0	75.3
FeedbackCNN	79.2	78.7	79.9	79.6	80.1

Table 1. Final test accuracies (%) across 5 runs on CIFAR-10. FeedbackCNN consistently achieves higher accuracy.

with top-down feedback, leading to iterative performance gains:

Refinement steps (T)	1	2	3	4	5
Test Acc.	78.5	79.6	80.1	80.5	80.8

Table 2. Effect of increasing the number of refinement iterations T on CIFAR-10 test accuracy. Gains begin to saturate after $T = 3$.

Though additional iterations do help, the marginal improvements diminish for $T > 3$. Even so, a few feedback iterations substantially boost accuracy, highlighting the value of top-down refinement.

4.3.1 ABLATION STUDY ON CIFAR-10

We also study how varying α (the feedback mixing parameter) and the dimensionality d_z of the feedback adapters affects performance as we increase T . Figure 6 shows a comparison of validation accuracy across different values of α and d_z . Each series reports performance at refinement steps $T = 1, 2, \dots, 5$.

As α increases, the model relies more heavily on top-down signals at each refinement step. We found that moderate values (e.g. $\alpha = 0.3$ and $d_z = 32$) strike a good balance between capacity and stability.

4.4 SpeechCommands with CNN and CFL

We further evaluate CFLs on the **SpeechCommands** dataset, which comprises one-second audio clips of spoken words. We convert raw audio waveforms into log-mel spectrograms and feed them into a small CNN, comparing a baseline CNN vs. **FeedbackCNN**.

Setup. We use 12 spoken-word classes, standard train/validation splits, and identical CNN backbones in both models aside from the CFL adapters.

Results. On the test set, the FeedbackCNN improves classification accuracy by over 1%, confirming that top-down feedback can also benefit audio tasks.

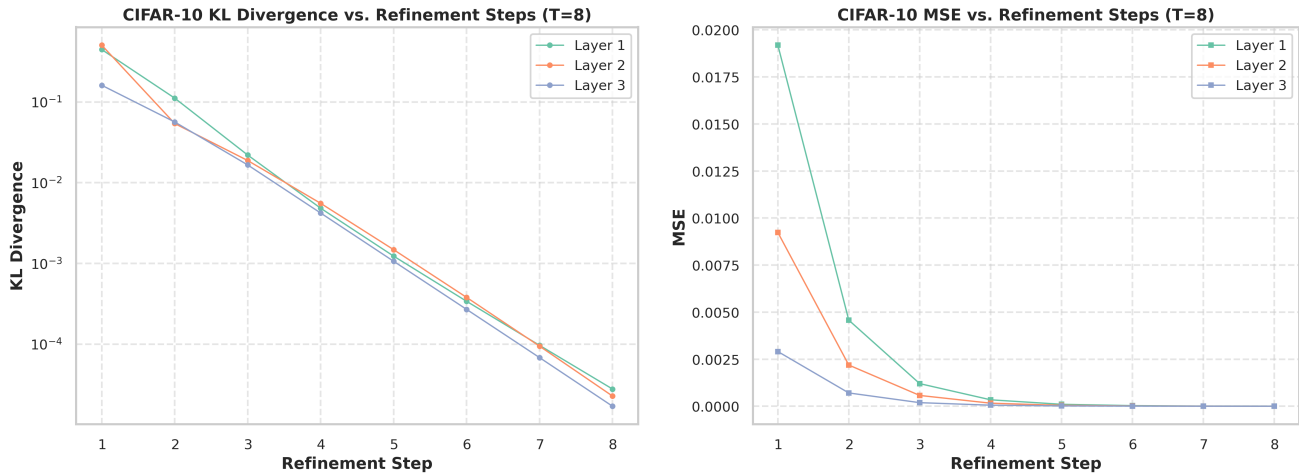
4.5 Scaling to ImageNet-1K with Vision Transformers

We now test CFLs on large-scale **ImageNet-1k** classification. We explore Vision Transformer (ViT) backbones of different scales:

Contextual Feedback Loops

Dataset	Model	Backbone Type	Depth	Heads	d_{model}	T
CIFAR-10	FeedbackCNN	CNN	3	–	–	Varies
SpeechCommands	FeedbackCNN	CNN	4	–	–	Varies
ImageNet-1K	FeedbackViT	ViT	12/24/32	12/16/16	768/1024/1280	2
GLUE (SST-2)	FeedbackTransformer	Transformer	12	12	768	1

Figure 3. **Hyperparameters.** Each dataset uses a distinct backbone architecture and set of hyperparameters. Here, T is the number of top-down refinements. On ImageNet-1K, we experiment with Base/Large/Huge variants of ViT, each having different depth, heads, and d_{model} . The GLUE benchmark is taken from (Wang et al., 2019).



(a) KL divergence between successive states. (Log scale on y-axis.)

(b) MSE between successive states.

Figure 4. **Refinement dynamics on CIFAR-10.** Each layer’s representation stabilizes after several feedback steps, as shown by decreasing KL divergence and MSE.

- **ViT-Base** (ViT-B/16),
- **ViT-Large** (ViT-L/16),
- **ViT-Huge** (ViT-H/14).

We compare each baseline (standard ViT) to its corresponding **FeedbackViT** (ViT + CFL).

Implementation details. We follow standard ViT training recipes, with patch embeddings, multi-head self-attention, and a feed-forward block repeated at varying depth. To enable feedback, each block has a small adapter and gating mechanism. We set $T = 2$ during training and inference. Table 3 summarizes the key hyperparameters.

Parameter and FLOP Costs. Table 3 shows that adding top-down feedback increases both parameter counts and FLOPs compared to the baseline ViT. The extra overhead arises primarily from:

- **Adapter modules:** small networks that project the top-down context.
- **Gating parameters:** additional learnable weights for modulating feedback signals.
- **Context vectors:** intermediate hidden states during feedback refinements.

While the overhead can be sizable for large transformers, it often remains acceptable in settings where model accuracy is critical.

Results. As summarized in Table 3, each FeedbackViT boosts top-1 accuracy over its baseline. Notably, **ViT-H + CFL** reaches 86.3% on ImageNet-1K (up from 85.7%). Hence, top-down refinement scales to large architectures, offering measurable gains despite increased computation.

Model	# Params (M)	FLOPs (G)	Top-1 (%)	Top-5 (%)
ViT-B/16 (baseline)	86.6	17.5	83.5	96.5
FeedbackViT-B/16	115.0	22.4	84.2	96.9
ViT-L/16 (baseline)	304.2	61.7	85.1	97.1
FeedbackViT-L/16	398.8	78.2	85.8	97.4
ViT-H/14 (baseline)	632.1	132.9	85.7	97.6
FeedbackViT-H/14	820.8	210.4	86.3	97.8

Table 3. **ImageNet-1K results** comparing baseline ViTs vs. FeedbackViTs. Adding top-down feedback increases parameters and FLOPs, but yields consistent gains in Top-1/Top-5 accuracy.

4.6 GLUE (SST-2) with a Transformer-based Backbone

Finally, we evaluate CFLs in a natural language processing context via the Stanford Sentiment Treebank (SST-2) por-

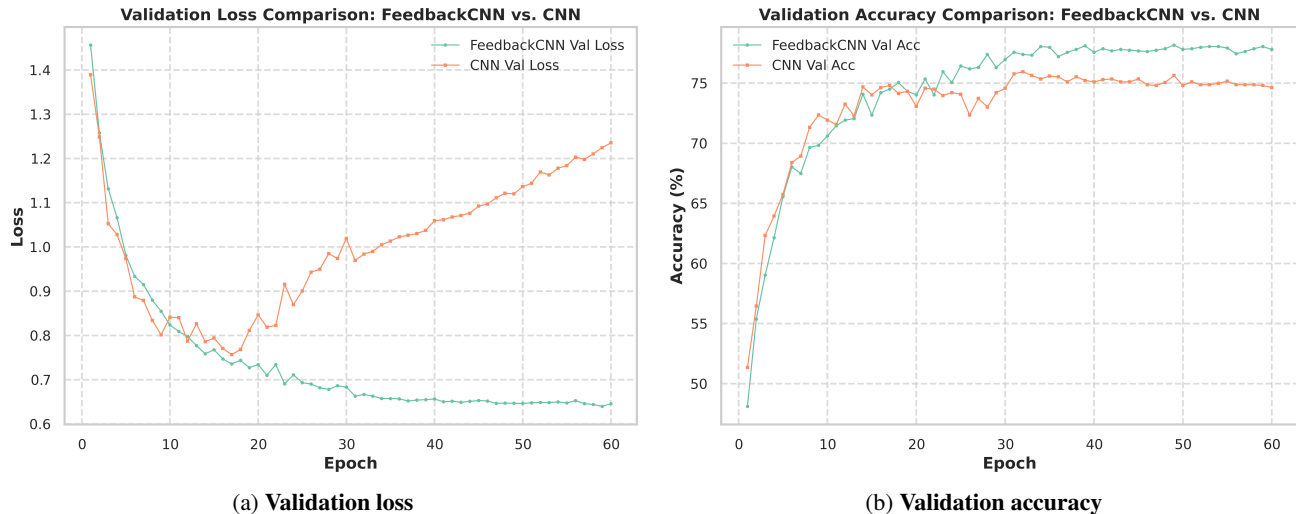


Figure 5. Training curves on CIFAR-10. **FeedbackCNN** achieves lower validation loss and higher accuracy compared to a baseline CNN.

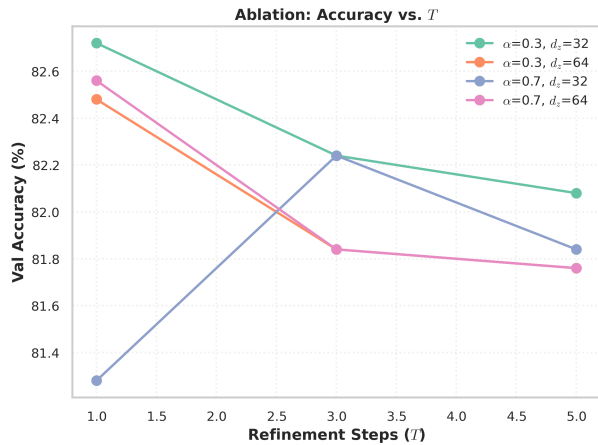


Figure 6. **Ablation on CIFAR-10.** We vary $\alpha \in \{0.3, 0.7\}$ and $d_z \in \{32, 64\}$ to measure validation accuracy at different numbers of refinement steps T . Moderate settings achieve the best overall results.

tion of the GLUE benchmark (Wang et al., 2019). We adopt a Transformer-based sequence classifier, comparing a baseline encoder-only Transformer vs. a **FeedbackTransformer** with the same hidden size and depth.

Setup. We tokenize input sentences and feed them into a 12-layer Transformer encoder, using the final [CLS] representation for classification. In the FeedbackTransformer, each layer is augmented with feedback adapters and a gating mechanism, with $T = 1$ refinement step.

Results. On the SST-2 dev set, the FeedbackTransformer improves classification accuracy by about 1.2% over the baseline, suggesting that top-down refinement can enhance NLP sentiment tasks, where global context helps refine token-level embeddings.

Dataset	Model Type	Baseline Acc.	Feedback Acc.	Δ
SpeechCommands	CNN	95.2%	96.3%	+1.1%
GLUE (SST-2)	Transformer	93.0%	94.2%	+1.2%

Table 4. **Results on SpeechCommands and GLUE (SST-2).** Our top-down feedback approach consistently outperforms the baseline models, yielding performance improvements in both tasks.

4.7 Summary of Empirical Findings

CFLs provide consistent improvements across vision (CIFAR-10, ImageNet-1K), audio (SpeechCommands), and NLP (SST-2) tasks, for both CNN and Transformer backbones. Even where top-down adapters introduce nontrivial overhead (e.g., large ViT models), the accuracy gains often justify this added cost. By stabilizing and refining hidden representations, top-down feedback helps mitigate ambiguity in lower layers and boost performance in a variety of domains.

5 Conclusion

We introduced **Contextual Feedback Loops (CFLs)** as a simple but broadly applicable way to fuse top-down context back into earlier layers of a neural network. Across several experiments, we found that a lightweight feedback path—projecting high-level outputs into a small context vector—can iteratively refine the internal representations in lower layers. This leads to improved accuracy, better stability, and more coherent hidden states.

References

Bai, S., Koltun, V., and Kolter, J. Z. Deep equilibrium models. In *Advances in Neural Information Processing*

- Systems (NeurIPS)*, pp. 690–701, 2019.
- Choksi, B., Mozafari, M., O’May, C. B., Ador, B., Alamia, A., and VanRullen, R. Predify: Augmenting deep neural networks with brain-inspired predictive coding dynamics, 2021. URL <https://arxiv.org/abs/2106.02749>.
- Elman, J. L. Finding structure in time. *Cognitive Science*, 14(2):179–211, 1990. doi: 10.1207/s15516709cog1402_1.
- Friston, K. The free-energy principle: a unified brain theory? *Nature Reviews Neuroscience*, 11(2):127–138, 2010.
- Gregor, K., Danihelka, I., Graves, A., and Wierstra, D. Draw: A recurrent neural network for image generation. In *Proceedings of the 32nd International Conference on Machine Learning (ICML)*, pp. 1462–1471, 2015.
- Grossberg, S. Towards solving the hard problem of consciousness: The varieties of brain resonances and the conscious experiences that they support. *Neural Networks*, 87:38–95, 2017. ISSN 0893-6080. doi: 10.1016/j.neunet.2016.11.003. URL <https://www.sciencedirect.com/science/article/pii/S0893608016301800>.
- Guo, Y., Lu, C., Allebach, J. P., and Bouman, C. A. Model-based iterative restoration for binary document image compression with dictionary learning, 2017. URL <https://arxiv.org/abs/1704.07019>.
- Hinton, G. E., Dayan, P., Frey, B. J., and Neal, R. M. The ‘wake-sleep’ algorithm for unsupervised neural networks. *Science*, 268(5214):1158–1161, 1995. doi: 10.1126/science.7761831.
- LeCun, Y., Bengio, Y., and Hinton, G. Deep learning. *Nature*, 521(7553):436–444, 2015. doi: 10.1038/nature14539.
- Lotter, W., Kreiman, G., and Cox, D. Deep predictive coding networks for video prediction and unsupervised learning. *arXiv preprint arXiv:1605.08104*, 2016.
- Rao, R. P. and Ballard, D. H. Predictive coding in the visual cortex: a functional interpretation of some extra-classical receptive-field effects. *Nature Neuroscience*, 2(1):79–87, 1999.
- Ronneberger, O., Fischer, P., and Brox, T. U-net: Convolutional networks for biomedical image segmentation. In *Medical Image Computing and Computer-Assisted Intervention (MICCAI)*, pp. 234–241, 2015.
- Sabour, S., Frosst, N., and Hinton, G. E. Dynamic routing between capsules. In *Advances in Neural Information Processing Systems (NeurIPS)*, pp. 3859–3869, 2017.
- Spoerer, C. J., McClure, P., and Kriegeskorte, N. Recurrent convolutional neural networks: A better model of biological object recognition. *Frontiers in Psychology*, 8:1551, 2017.
- Spratling, M. W. A review of predictive coding algorithms. *Brain and Cognition*, 112:92–97, 2017. doi: 10.1016/j.bandc.2015.11.003.
- Wang, A., Singh, A., Michael, J., Hill, F., Levy, O., and Bowman, S. R. Glue: A multi-task benchmark and analysis platform for natural language understanding, 2019. URL <https://arxiv.org/abs/1804.07461>.
- Wen, L., Du, D., Cai, Q., Lei, Z., Hung, T.-J., Senior, A., and Lyu, S. Recurrent attentive zooming for joint crowd counting and precise localization. In *IEEE Conference on Computer Vision and Pattern Recognition (CVPR)*, pp. 1217–1226, 2018.
- Zamir, A. R., Wu, T.-L., Sun, L., Shen, W. B., Malik, J., and Savarese, S. Feedback networks. In *Proceedings of the IEEE Conference on Computer Vision and Pattern Recognition (CVPR)*, pp. 1308–1317, 2017.